

RESEARCH ARTICLE

Vascular age estimation using a consumer wearable sleep tracker

Gizem Yilmaz¹, Shohreh Ghorbani¹, Ju Lynn Ong¹, Hosein Aghayan Golkashani¹, Chen Zhang^{1,2,3}, B. T. Thomas Yeo^{1,2,3,4,5,6,7}, Michael W. L. Chee^{1,2*}

1 Centre for Sleep and Cognition, Yong Loo Lin School of Medicine, National University of Singapore, Singapore, Singapore, **2** Centre for Translational Magnetic Resonance Research (TMR), Yong Loo Lin School of Medicine, National University of Singapore, Singapore, Singapore, **3** Department of Electrical and Computer Engineering, National University of Singapore, Singapore, Singapore, **4** N.1 Institute for Health and Institute for Digital Medicine (WisDM), National University of Singapore, Singapore, Singapore, **5** Integrative Sciences and Engineering Programme (ISEP), National University of Singapore, Singapore, Singapore, **6** Healthy Longevity Translational Research Programme & Human Potential Translational Research Programme, Yong Loo Lin School of Medicine, National University of Singapore, Singapore, Singapore, **7** Martinos Center for Biomedical Imaging, Massachusetts General Hospital, Boston, Massachusetts, United States of America

☞ These authors contributed equally to this work.

* michael.chee@nus.edu.sg



OPEN ACCESS

Citation: Yilmaz G, Ghorbani S, Ong JL, Golkashani HA, Zhang C, Yeo BTT, et al. (2026) Vascular age estimation using a consumer wearable sleep tracker. PLOS Digit Health 5(3): e0001329. <https://doi.org/10.1371/journal.pdig.0001329>

Editor: Shrey Lakhotia, Henry Ford Health System, UNITED STATES OF AMERICA

Received: August 4, 2025

Accepted: March 11, 2026

Published: March 30, 2026

Copyright: © 2026 Yilmaz et al. This is an open access article distributed under the terms of the [Creative Commons Attribution License](https://creativecommons.org/licenses/by/4.0/), which permits unrestricted use, distribution, and reproduction in any medium, provided the original author and source are credited.

Data availability statement: Aggregated participant-level data for Fingertip and Ring devices used to generate tables and figures are available at <https://github.com/SCL-NUS/ppg-vascularage-ring>. Fingertip PPG waveform data, including all waveforms from each night's recording as well as the exact subset used for

Abstract

Vascular aging is traditionally assessed using a combination of clinical markers, blood pressure and arterial stiffness measurement. However, measuring vascular aging with reference equipment is costly and not scalable. Nocturnal photoplethysmography (PPG) from wearable health trackers offer a scalable solution for longitudinal assessment. In this study, we evaluated the ability of a consumer wearable (Oura Ring) to detect age-related differences in PPG waveform, in comparison to a clinical-grade fingertip pulse oximeter. Healthy adults (N = 160; 78 males (49%), median age 31 years (IQR: 23)) underwent overnight polysomnography (PSG) in a sleep laboratory, during which fingertip and wearable ring PPG data were collected simultaneously. Pulse waveforms were extracted from both devices using a custom algorithm and key waveform features were compared across devices. Vascular age was estimated from pulse waveforms using a featureless deep learning model. Prediction performance was compared between the two devices. Age-related waveform changes were most prominent in PPG crest time (CT (samples)) ($r=0.64$ and 0.62 for fingertip and wearable devices), while the reflection index (RI) had a weaker correlation with age for the ring sensor ($r=0.22$) compared to fingertip ($r=0.58$). Despite differences in waveforms between devices, the deep learning model showed comparable prediction performance with mean absolute errors (MAE (SD)) of 6.28 (1.48) and 7.25 (1.29) years, and r (SD) of 0.84 (0.07) and 0.80 (0.10) for clinical-grade and consumer-grade devices, respectively. These findings support the feasibility of using PPG waveforms from wearable devices to assess vascular age.

model training and evaluation, can be accessed via OSF repository (<https://doi.org/10.17605/OSF.IO/7TZCG>). The Oura PPG waveform data cannot be publicly available due to contractual agreements between National University of Singapore and Oura Health Oy.

Funding: This work was supported by the Lee Foundation (wearelee.org/lee-foundation), Support funds for the Centre for Sleep and Cognition, Yong Loo Lin School of Medicine (medicine.nus.edu.sg) awarded to Michael W. L. Chee. All grants were awarded to Michael W. L. Chee. The funders had no role in the design of the study; in the collection, analyses, or interpretation of data; in the writing of the manuscript; or in the decision to publish the results.

Competing interests: I have read the journal's policy and the authors of this manuscript have the following competing interests: Michael W. L. Chee is a member of the medical advisory board of Oura Health. As of October 2025, Gizem Yilmaz and Ju Lynn Ong are members of the Oura–National University of Singapore (NUS) Joint Lab. This work was conducted independently of Oura Health and the Joint Lab, and was designed, funded, and executed solely by NUS. Oura Health had no role in data analysis, interpretation or in the writing of the manuscript. The manuscript was submitted on August 4, 2025. No other disclosures were reported.

Author summary

Vascular aging is an important marker of cardiovascular risk, traditionally assessed using clinical measurements and specialized equipment to evaluate arterial stiffness. The latter is expensive and difficult to scale for long-term or population-level monitoring. Wearable health trackers that collect nocturnal photoplethysmography (PPG) signals offer an alternative. Our study examined whether a consumer wearable device (Oura Ring) can detect age-relevant features in PPG waveforms, compared with a clinical-grade fingertip pulse oximeter. 160 healthy adults (49% male; median age 31 years) underwent overnight polysomnography, during which PPG signals were recorded simultaneously from both devices. Pulse waveforms were extracted and key waveform features were analyzed. Several PPG features showed clear age-related changes, particularly pulse crest time, which correlated strongly with age for both devices. Vascular age was then estimated using a deep-learning model applied to the PPG signals. Although waveforms differed between devices, the deep-learning model predicted vascular age with comparable accuracy using wearable and clinical-grade PPG data. Mean absolute error was approximately 6–7 years for both devices, with strong correlations between predicted and chronological age. These findings demonstrate that PPG data from consumer wearables can capture meaningful age-related vascular information, supporting their potential use for scalable, longitudinal assessment of vascular aging.

Introduction

Modifying lifestyle risk factors is important for the prevention of cardiovascular disease, the leading cause of death in industrialized societies [1]. Vascular aging refers to age-related changes in the structure and function of the arterial system, and is an important marker of cardiovascular disease (CVD) risk [2–4]. Arterial stiffness and blood pressure, two key determinants of vascular aging, both tend to increase with age [5–8]. Unhealthy lifestyles and/or environmental agents can accelerate vascular aging [9–11]. Conversely, premature vascular aging may be mitigated through improving diet and aerobic exercise [9]. To reinforce desirable behavioural change, it would be useful to provide individuals with regular, accurate feedback through wearable health trackers, in much the same way that continuous performance monitoring has transformed sport performance.

Vascular age is commonly estimated through a vascular risk profile that incorporates established biomarkers such as blood pressure and serum lipid levels, along with arterial stiffness. Arterial stiffness is most commonly assessed as carotid–femoral pulse wave velocity (cfPWV) using applanation tonometry [2,12]. A gap between vascular and chronological age suggests early or accelerated vascular aging [3]. More recently, vascular age has been predicted using only tonometer derived arterial pulse waveforms, analyzed with a deep learning model. Vascular age predicted in

this manner showed strong association with the risk of adverse cardiovascular events [13]. While this latter study demonstrated the value of analyzing arterial waveforms, a tonometry-based approach uses costly, specialized equipment and is impractical for long-term, longitudinal monitoring of arterial stiffness at scale. Approaches that enable frequent and longitudinal assessment could enhance the early identification of persons at increased risk of cardiovascular disease [4].

Wearable fitness and sleep trackers equipped with high-quality photoplethysmography (PPG) sensors are good candidates for large-scale continuous monitoring of cardiovascular health [14]. Currently, these devices primarily use PPG signals to measure pulse rate and pulse rate variability. However, high fidelity PPG waveforms can also be used to infer arterial stiffness and its age-related change [15–17]. This represents a major opportunity to longitudinally evaluate vascular health [18] and how lifestyle changes might affect arterial stiffness.

The contour of the pulse waveform, both arterial and PPG-based, changes with chronological age, as increased arterial stiffness leads to faster pulse wave propagation and enhanced wave reflection from the periphery [19,20]. With increasing age, the PPG waveform exhibits rounder systolic peaks with a lower slope, along with a less pronounced or absent dicrotic notch [15,16,21–25]. This and other PPG waveform features have been proposed to assess vascular age [26], and have been utilized in regression-based models for this purpose [27–31]. Such feature-based models rely on accurate fiducial point detection, which may be compromised by distortions in the pulse contour. An alternative is to directly feed pulse waveforms into deep learning models, which can overcome challenges in feature extraction and have demonstrated superior prediction of vascular aging compared to feature-based models [32–34]. A recent landmark study using a PPG-based deep learning framework reported associations between smartwatch-derived PPG estimates and health-related outcomes, illustrating the potential for real-world application [35]. However, PPG waveforms differ across recording site and device used and understanding which PPG features contribute to age prediction is helpful in giving insight into the underlying physiological changes that drive vascular age prediction.

In this work, we evaluated the feasibility of using a ring-based consumer device (Oura Ring) to assess vascular age using PPG waveforms and compared its performance to that of a clinical-grade, fingertip PPG sensor. Specifically, we tested whether ring derived PPG signals can comparably estimate vascular age to fingertip PPG whose signal waveforms are most familiar to clinicians. Critically, while both assess PPG at the finger, waveforms differ when obtained from the fingertip and around the finger. Assessments were conducted during sleep, which is associated with much reduced motion signal artifacts [36]. We first compared the pulse waveforms from two devices and characterized their differences. Next, we assessed the association strength between age and selected PPG waveform features. Finally, we predicted vascular age from pulse waveforms using deep learning and compared the prediction performance between the two devices.

Results

We studied nominally healthy adults from 20 to 70 years of age who were mostly normotensive and whose characteristics are summarized in [Table 1](#). 158 participants contributed to the PPG feature-based analysis and 160 to the deep learning prediction of vascular age.

Pulse waveform similarity between fingertip device and wearable ring

To determine if the wearable device retained essential pulse contour characteristics necessary for detection of relevant hemodynamic features, waveform similarity between the fingertip device and the ring pulses was evaluated ([Fig 1](#)).

The median (IQR) cross-correlation value of PPG waveforms across all participants was 0.97 (0.02) indicating overall high similarity between devices ([Fig 2a](#)). Average waveforms for the fingertip sensor and ring showed that the timing of systolic and diastolic peaks were mostly aligned, with the ring having a rounder systolic peak ([Fig 2b](#)). However, the amplitude of the diastolic phase and peak was noticeably higher in the ring compared to the fingertip sensor. With increasing age, this systolic peak showed a rounder morphology with a shift in timing, while the diastolic peak gradually flattened, giving the waveform a more blunted appearance in both devices ([Fig 2c](#)).

Table 1. Demographic summary of samples used in PPG feature-based analysis and deep-learning based age prediction model.

Characteristic	PPG feature-based, N=158	Deep-learning based, N=160
Age (years)	31 (25)	31 (23)
20-39	108 (68.3%)	109 (68.1%)
40-59	32 (20.3%)	33 (20.6)
≥60	18 (11.4%)	18 (11.3)
Sex (n(%))		
Male	76 (48%)	78 (49%)
Female	82 (52%)	82 (51%)
BMI (kg/m²)	22.8 (3.8)	22.8 (3.9)
SBP (mmHg)	112 (18.9)	112 (18.7)
DBP (mmHg)	71 (10.5)	71 (10.4)

Median (IQR); n (%); SBP: Systolic Blood Pressure; DBP: Diastolic Blood Pressure

<https://doi.org/10.1371/journal.pdig.0001329.t001>

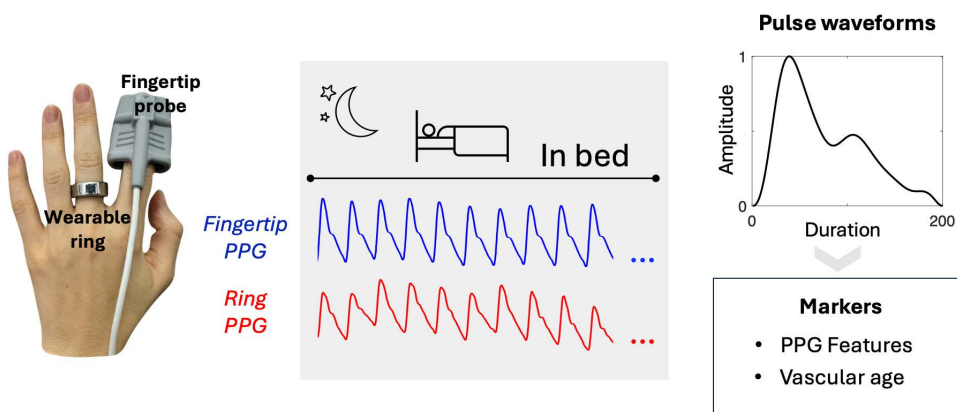


Fig 1. Illustration of devices, protocol and main outcomes. During sleep, participants underwent simultaneous PPG recordings using both a clinical-grade pulse oximeter (Fingertip probe) and a consumer wearable ring (Oura Ring). The data were analysed to assess PPG waveform characteristics and predict vascular age.

<https://doi.org/10.1371/journal.pdig.0001329.g001>

Quantifying waveform differences using PPG features

Differences in waveforms between the fingertip sensor and ring were quantified using PPG features with values summarized in [Table 2](#). Values of CT and RI differed between the devices, with the ring showing higher values. In contrast, dT did not differ significantly between the fingertip and the ring. In distribution plots, RI showed the largest difference in magnitude, with a clear separation between devices ([S1 Fig](#)). Additionally, when PPG features were not-normalized for duration, CT (seconds) was significantly higher in the ring, while values for dT (seconds) were similar ([S1 Table](#)).

To examine the noise inherent in the PPG feature extraction process, we measured the agreement in PPG features between the two devices ([Table 3](#)). CT had the highest agreement between devices with correlation coefficient of 0.8, with a positive bias of 6.05 (6.16) samples indicating an overestimation for the ring. The dT and RI had similar (moderate) levels of agreement with a correlation value around 0.5, while ring overestimated RI (bias of 0.23 (0.1); [S2 Fig](#)). The degree of agreement and bias were similar for un-normalized PPG features, CT (seconds) and dT (seconds). CT (seconds) showed the best agreement between devices ([S2 Table](#)).

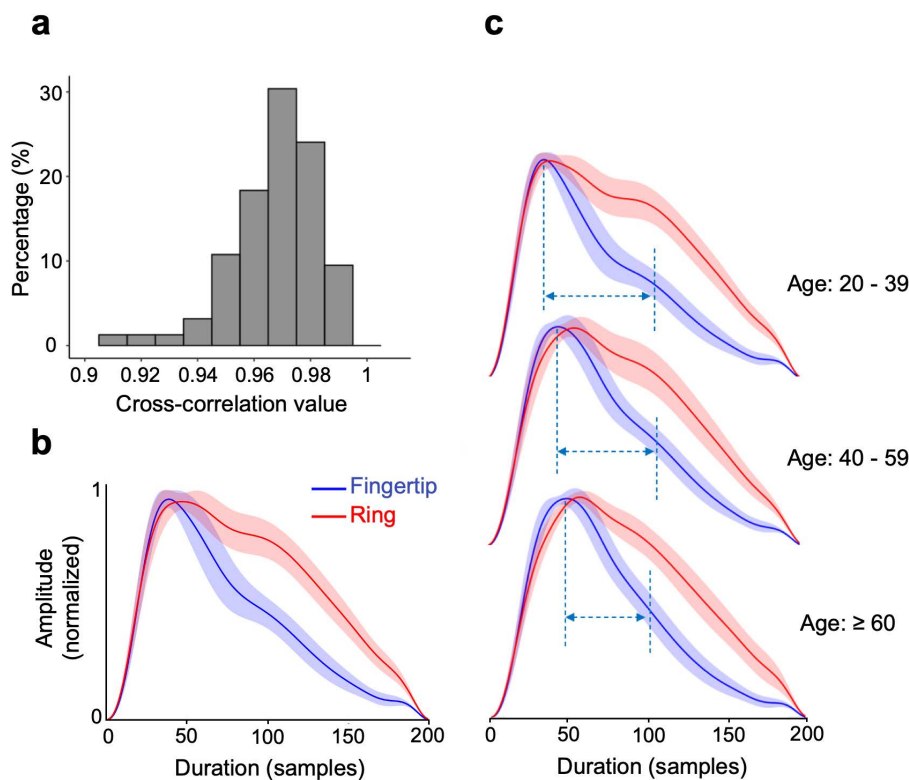


Fig 2. Pulse waveform similarity between the fingertip sensor and the wearable ring. a. Distribution of cross-correlation coefficients between devices for all participants. b. Average waveforms (derived from all participants) from Fingertip (blue) and Ring (red). Shaded areas show standard deviation at each sample point. c. Average pulse waveforms for three age groups: 20-39, 40-59, and 60 and above. Vertical dashed blue lines indicate systolic and diastolic peak locations on Fingertip pulse; horizontal dashed lines show approximate distance between 2 peaks.

<https://doi.org/10.1371/journal.pdig.0001329.g002>

Table 2. Summary of PPG-features from the fingertip sensor and the ring.

PPG feature	Fingertip, N = 158 ¹	Ring, N = 158 ¹	p-value ²
CT (samples)	38.7 (9.4)	45.0 (15.3)	<0.001
dT (samples)	60.3 (10.6)	58.8 (10.9)	0.6
RI (ratio)	0.54 (0.17)	0.78 (0.12)	<0.001

¹Median (IQR), ²Wilcoxon rank sum test.

CT: Crest time, dT: distance between systolic and diastolic peaks, RI: Reflection index

<https://doi.org/10.1371/journal.pdig.0001329.t002>

Table 3. Agreement between PPG-features extracted from the fingertip sensor and the ring.

PPG feature	Bias ^{1,2}	[Lower LoA, Upper LoA]	Correlation
CT (samples)	6.05 (6.16)	[-6.02, 18.11]	0.8
dT (samples)	-0.78 (7.98)	[-16.41, 14.86]	0.54
RI (ratio)	0.23 (0.10)	[0.04, 0.42]	0.54

¹Mean (SD), ² Bias: the difference between the ring and fingertip sensor.

LoA: Limits of Agreement, CT: Crest time, dT: distance between systolic and diastolic peaks, RI: Reflection index.

<https://doi.org/10.1371/journal.pdig.0001329.t003>

Chronological age and pulse waveform relationship

The linear relationship between chronological age and PPG features was in the expected direction for both devices (Fig 3). The strongest correlation with age was observed for CT with coefficients of 0.64 ($p < 0.001$) and 0.62 ($p < 0.001$) for fingertip and ring devices, respectively. Association with age was moderate for dT ($r = -0.51$, $p < 0.001$) for both devices. The largest discrepancy between devices was observed for RI, as correlation was 0.58 ($p < 0.001$) for the fingertip sensor and 0.22 ($p < 0.001$) for the ring. The difference in correlation strength between the two devices was significant only for RI (Fisher's z test $p < 0.05$). The observed associations for PPG features and devices remained significant after correcting for sex, BMI, SBP and DBP except for RI from the ring (S3 Table). The current subset of randomly sampled windows was representative of participant means, as the correlation with age was comparable across 100 different window subsets (S3 Fig).

Lastly, in regression models predicting vascular age using CT, dT and RI alone, there was no statistical difference between prediction performance between the fingertip device and the ring (S4 Table). The regression model had a mean absolute error (MAE) of 7.76 ± 1.49 years (mean \pm SD) for the fingertip device and 8.95 ± 1.54 years for the ring. The root mean square error (RMSE) was slightly lower for the fingertip device at 9.69 ± 2 years compared to 10.8 ± 1.9 years for the ring. Both devices showed moderate correlations between predicted and actual age, with correlation coefficients (r) of 0.77 ± 0.11 for the fingertip device and 0.70 ± 0.14 for the ring. Finally, R^2 values were 0.60 ± 0.17 for the fingertip device and 0.52 ± 0.2 for the ring.

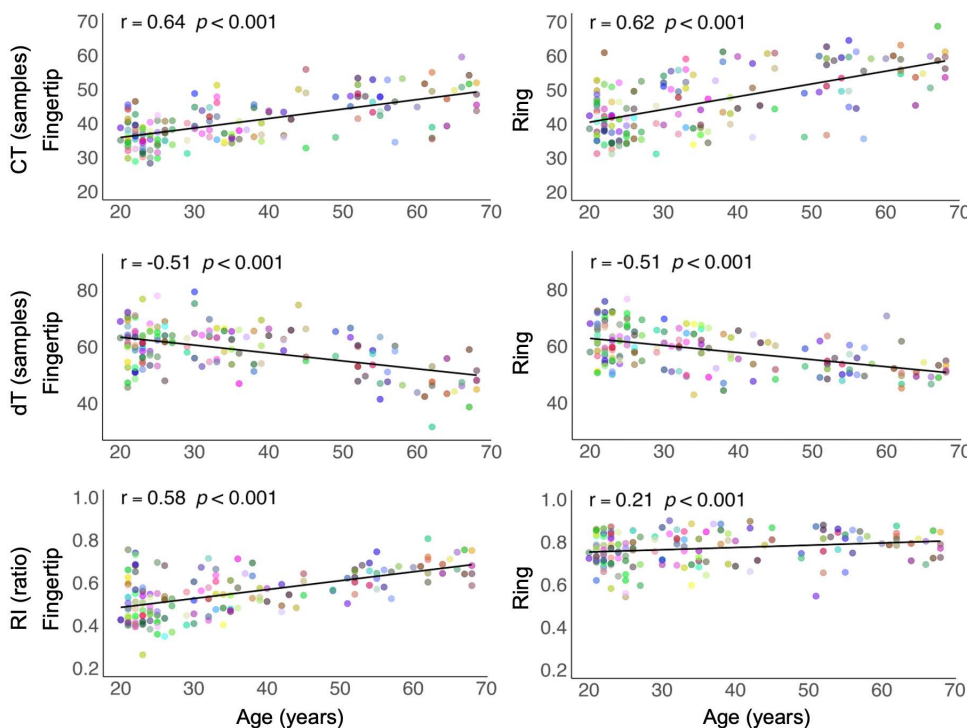


Fig 3. Linear relationship between age and PPG features. Scatter plots for Fingertip (left column) and Ring (right column) for CT (Crest time), dT (distance between systolic and diastolic peaks), and RI (Reflection index). Each color (point) is a different participant.

<https://doi.org/10.1371/journal.pdig.0001329.g003>

Age prediction via deep-learning model

Vascular age prediction performance of deep learning model (CNN) was similar between the fingertip device and the ring, with the fingertip device showing numerically slightly lower MAE and higher R^2 and r values (Table 4). The CNN model achieved a mean absolute error (MAE) of 6.28 ± 1.48 years (mean \pm SD) for the fingertip device and 7.25 ± 1.29 years for the ring. The root mean square error (RMSE) was slightly lower for the fingertip device at 8.01 ± 1.83 years compared to 9.07 ± 1.91 years for the ring. Both devices demonstrated strong correlations between predicted and actual age, with correlation coefficients (r) of 0.84 ± 0.07 for the fingertip device and 0.80 ± 0.1 for the ring. Similarly, R^2 values were 0.67 ± 0.11 for the fingertip device and 0.59 ± 0.15 for the ring, indicating robust predictive performance. After adjusting for multiple comparisons, none of the differences were statistically significant between the two devices (S4 Fig and S5 Table).

The agreement between actual and estimated age was high for both devices, with strong correlations across the 10 folds ranging from $r=0.69$ to $r=0.97$ for the fingertip device, and $r=0.63$ to $r=0.89$ for the ring (Fig 4a). In Bland Altman plots, the mean bias (SD) was small (Fingertip: -0.75 (8.25) years, Ring: -1.31 (9.15) years) (Fig 4b). However, a pattern of proportional bias was observed with increasing age, indicating underestimation in older participants and overestimation in younger participants. The bias (raw Δ Age) was significantly associated with chronological age for both devices, with slopes [95% CI] of -0.39 [$-0.45, -0.33$] for the fingertip and -0.46 [$-0.50, -0.40$] for the ring across all folds. To visualize age-independent residual variability, age-adjusted Δ Age values are additionally presented in Fig 4c. These adjusted Bland Altman plots are intended for the characterization of variability in age-independent Δ Age values and not to assess absolute agreement.

Key regions of the PPG waveform for CNN model

Grad-CAM visualizations showed that areas of importance vary with age, with a diminished focus near the pulse onset and an expansion of intermediate-level importance regions in older age groups (ages over 60). These trends were observed for both the fingertip and the ring, suggesting that both devices capture sufficient signal features for age prediction (Fig 5).

Associations of Δ Age with blood pressure

Model-adjusted SBP increased with increasing Δ Age grouped into tertiles (Fig 6A). For fingertip PPG, participants in the third (highest) tertile of Δ Age (T3) had significantly higher SBP than those in the first (lowest) tertile (T1) (mean difference = 6.11 mmHg, SE = 2.37 , $p=0.032$), while differences between T1–T2 and T2–T3 were not statistically significant. For ring PPG, compared with the first Δ Age tertile (T1), model-adjusted SBP was higher in both the second (T2; mean difference = 5.65 mmHg, $p=0.048$) and third tertiles (T3; mean difference = 8.00 mmHg, $p=0.003$). T2 and T3 did not differ significantly. Although DBP showed an increasing trend across Δ Age tertiles for both Fingertip and Ring, pairwise comparisons did not show statistically significant differences between groups (Fig 6B).

Table 4. Age prediction performance for the fingertip sensor and the ring.

	Fingertip, N = 160 ¹	Ring, N = 160 ¹	p-value
MAE	6.28 (1.48)	7.25 (1.29)	0.080
RMSE	8.01 (1.83)	9.07 (1.91)	0.186
R ²	0.67 (0.11)	0.59 (0.15)	0.179
r	0.84 (0.07)	0.80 (0.10)	0.263

¹Mean (SD), MAE: Mean absolute error, RMSE: Root mean squared error, R²: Coefficient of determination, r: Correlation coefficient

<https://doi.org/10.1371/journal.pdig.0001329.t004>

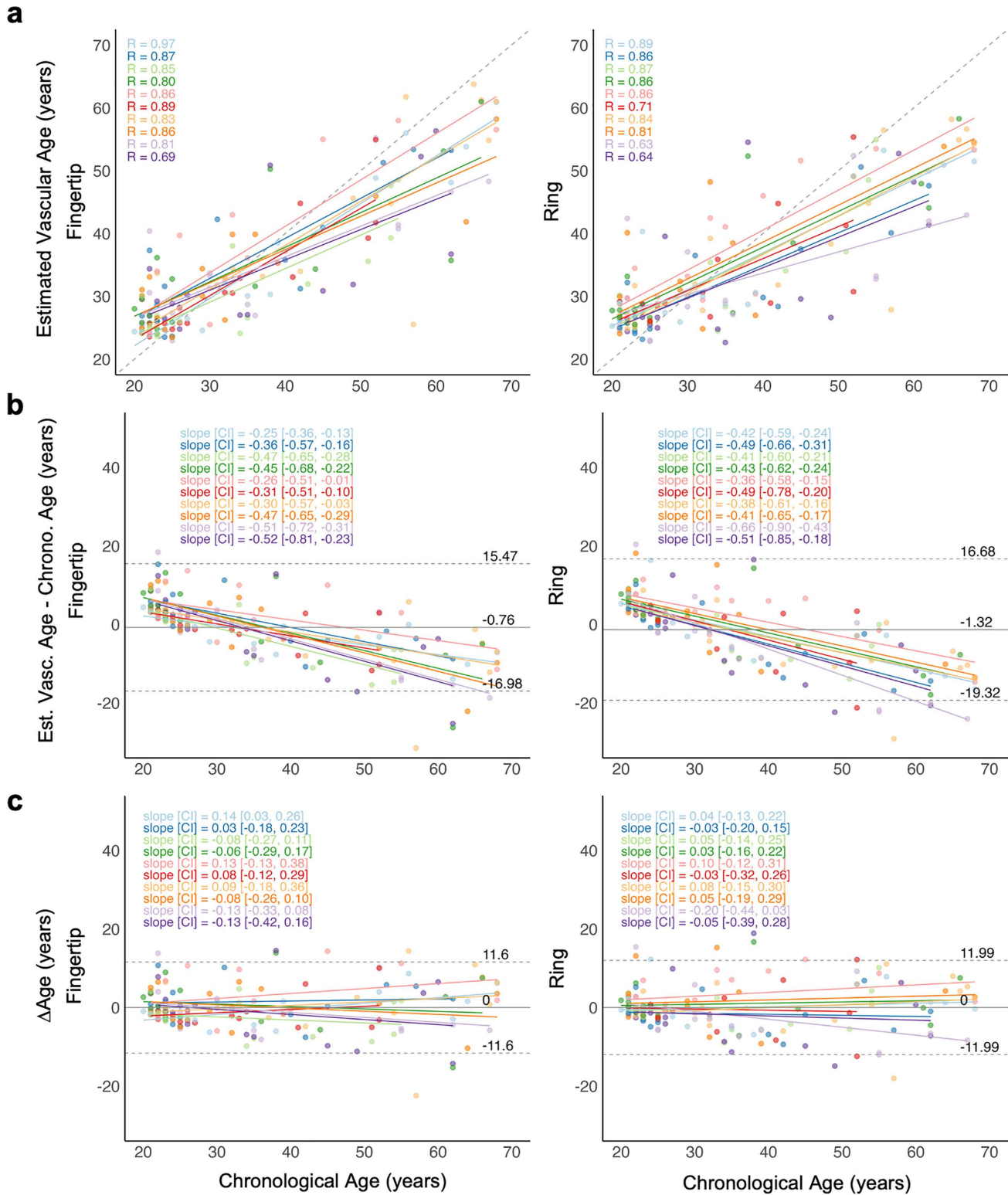


Fig 4. Agreement between the chronological age and estimated vascular age. **a.** Scatter plot of estimated vascular age versus chronological age across cross-validation folds for all subjects for Fingertip (left column) and Ring (right column) (N = 160). Each color represents a fold, with solid lines showing fold-specific regression fits. The dashed gray line marks perfect estimation (identity line). R: Pearson's correlation coefficient. **b.** Bland-Altman plot comparing estimated vascular age to chronological age. The solid grey line shows mean difference, with 95% confidence intervals (dashed grey

lines) representing the limits of agreement. Fold-specific regression lines and their slope and 95% CI are shown via different colors. c. Age-adjusted Δ Age values across chronological age after proportional bias removal. Fold-specific regression lines and their slope and 95% CI are shown via different colors.

<https://doi.org/10.1371/journal.pdig.0001329.g004>

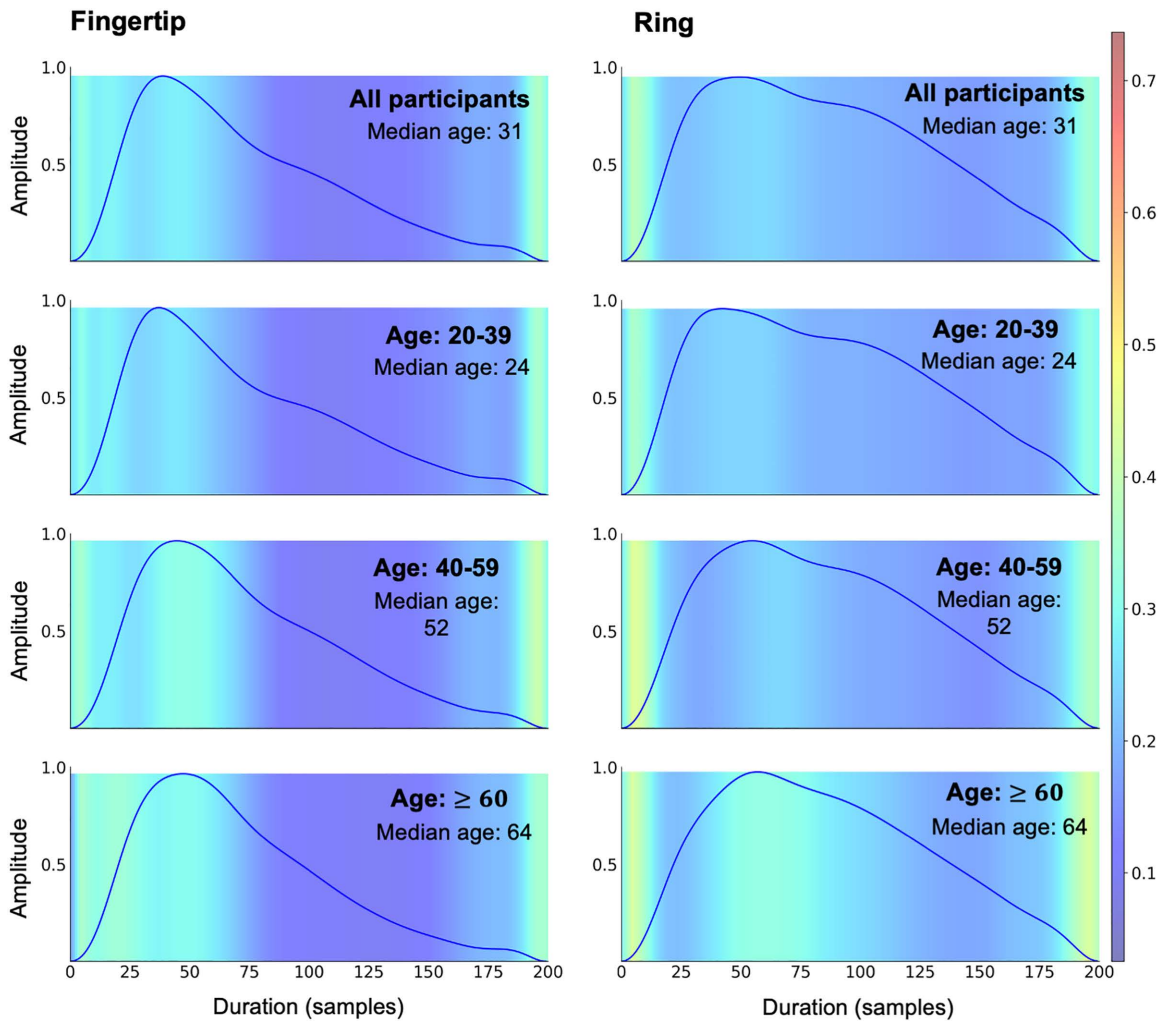


Fig 5. Important regions of the PPG waveform for CNN model. Grad-CAM visualizations of PPG waveforms using Fingertip (left) and Ring (right) devices. Results are displayed for different age groups across rows. Top row: all participants included, second row: ages 20–39, third row: ages 40–59, and bottom row: ages 60 and above. The colour intensity reflects the model's attention, with warmer colours (yellow) indicating areas of higher relevance in age estimation. Across both devices, the focus areas shift with increasing age, highlighting broader regions of intermediate importance in older age groups.

<https://doi.org/10.1371/journal.pdig.0001329.g005>

Discussion

We found that photoplethysmography (PPG) signals from a ring-based consumer device can assess vascular age as well as a clinical-grade fingertip sensor. The pulse waveforms from the ring were of comparable quality to those from the fingertip device, despite differences in pulse contours between devices. We observed moderate to high correlations with age for CT, dT, and RI when using the fingertip probe. The strength of the correlations was similar for the ring, except for RI,

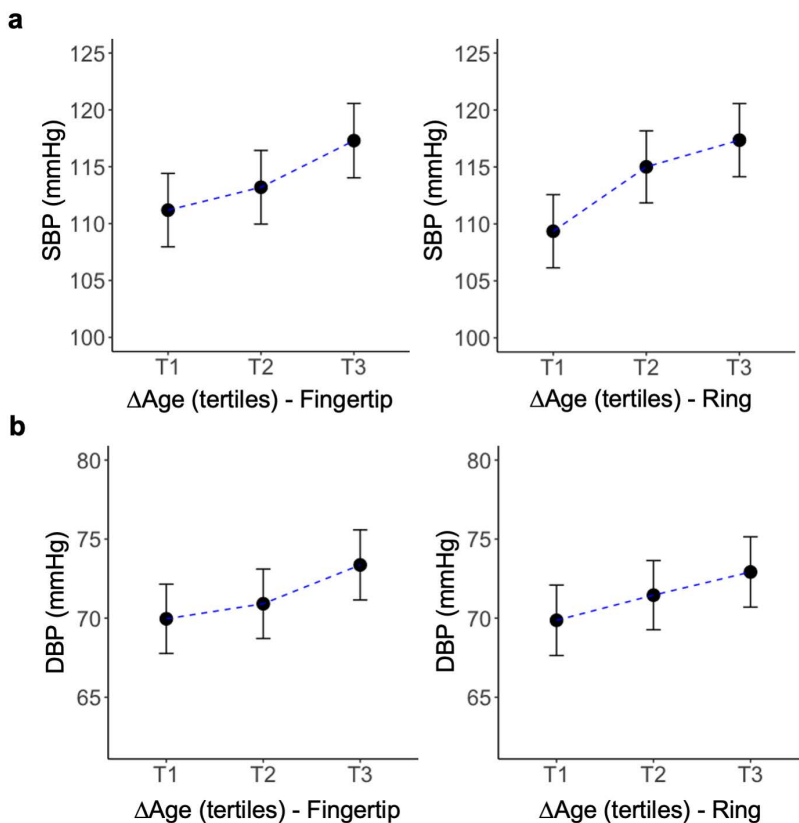


Fig 6. Model-adjusted systolic blood pressure (SBP) (a) and diastolic blood pressure (DBP) (b) across Δ Age tertiles derived from Fingertip and Ring. Points represent estimated marginal means from regression models adjusted for age, sex and BMI; error bars indicate 95% confidence intervals. Blue dashed lines show trend. Δ Age values are age-adjusted. Mean Δ Age for T1, T2, and T3 was -5.9 , -0.5 , and 6.5 years for Fingertip and -6.1 , -0.4 , and 6.6 years for Ring, respectively.

<https://doi.org/10.1371/journal.pdig.0001329.g006>

which had a weaker correlation with age. Finally, we predicted vascular age for both devices using raw pulse waveforms in a CNN model, achieving similar performance for both wearable and fingertip devices suggesting that the wearable ring can assess age-related changes in arterial stiffness, comparable to a fingertip sensor.

Comparing fingertip and ring derived PPG waveforms

The observed differences in pulse waveforms between devices were primarily driven by the interdependent effects of measurement site, sensor mode and design. The ring-based wearable device used in this study measures PPG on the palmar side at the base of the finger, an area with fewer capillaries and branching arteries compared to the fingertip [37], which likely reduces sensitivity to blood volume changes and contributes to delayed systolic peak timing (i.e., a greater CT value) and a higher diastolic amplitude (i.e., a greater RI). Despite the short distance between the fingertip and the base of the finger, increased reflection at the base may have also contributed to diastolic amplification and delayed systolic timing, compared to the fingertip [38]. Additionally, the ring's rigid form may increase contact pressure during sleep when hand swelling occurs [39], causing greater variability in temporal features (including CT and dT) with increasing contact pressure levels [40]. Lastly, the fingertip device used in this study utilized a conventional transmission-type pulse oximeter, whereas the consumer wearable uses multiple infrared LEDs in both reflectance

and transmission modes to collect PPG during sleep [41]. However, a comprehensive evaluation of the effect of sensor mode on pulse contour is still needed.

With age, increased arterial stiffness leads to faster pulse wave propagation, reduced compliance of smaller peripheral arteries, and increased wave reflection [19], which in turn augments systolic pressure, steepens the upstroke, and flattens or blunts the dicrotic notch. While many features can be derived from PPG pulse waveforms, we focused on CT, dT, and RI to capture age-related changes, as these features are strongly linked to age related vascular stiffening [15,16,21–24,31,42], and are straightforward to interpret. Both the fingertip device and the ring showed a similar degree of linear association between age and CT, consistent with studies using data from the fingertip [15,23]. In contrast, the correlation for RI from the ring was significantly weaker than that from the fingertip, with only the latter consistent with previous reports [22]. The rigid structure of the ring may have caused variations in contact pressure throughout the night, potentially reducing RI's sensitivity [40].

PPG-based vascular age estimation models

Despite the utility of PPG features for evaluating blood vessel elasticity [26], there is currently no consensus or established guidelines on the most informative pulse characteristics for assessing vascular age. This lack of standardization becomes evident in the heterogeneity of the number and combinations of pulse waveform features used in vascular age prediction studies [30,31,33,43]. Feature-based models require precise fiducial point detection, which distortions in the pulse contour can compromise. In individuals with multiple risk factors or established cardiovascular disease, stiff arteries cause the reflected wave to merge with the direct wave, obscuring fiducial points [44]. Extracted PPG features may be even noisier with wearable data collected in real-world settings.

Using extracted pulse waveforms directly in a deep learning model may circumvent some inherent limitations of PPG feature extraction. As expected, the CNN model had better prediction performance than the PPG feature-based regression model (S5 Fig), although a more detailed comparison between the two models is beyond the scope of the current work. Nonetheless, both models showed similar performance across the two devices, and to our knowledge, these are the first findings to demonstrate that wearable PPG signals can achieve accuracy comparable to fingertip PPG in vascular age prediction. Previous deep learning studies have predicted vascular age using single-site PPG from the finger [33] and nasal cavity [30,43], multiple-site PPG from the finger, wrist, arm, and ankle [32], as well as brachial, radial, and carotid tonometry waveforms [13]. Our CNN model achieved smaller prediction errors and higher correlations than previous studies using single-site PPG [34,43], though direct comparisons are limited by differences in datasets (e.g., wake vs. sleep, sensor mode) and preprocessing pipelines. While the CNN model eliminated the need for manual feature engineering, Grad-CAM visualizations revealed that both devices relied on similar waveform regions to derive vascular age information, emphasizing consistent feature importance across devices. Notably, these highlighted regions (from onset to the dicrotic notch) align with the vascular aging characteristics of waveforms described earlier. Despite the attenuated age-related association observed for RI in the ring sensor, the CNN model captured vascular age information by leveraging the full waveform characteristics.

Broadening the application of vascular age measurement to health monitoring

Tonometer based vascular age inference [2–4,12] is mostly confined to specialized clinics, involving infrequent measurements performed on individuals already at risk or who have cardiovascular disease. In contrast, wearable-based arterial health assessments provide a convenient means for the collection of frequent samples in the field. As these devices are widely accessible and affordable, they may prove invaluable in providing feedback about how lifestyle choices affect arterial stiffness.

Overall, our findings suggest that consumer wearables collecting high fidelity PPG data, like the Oura ring, can capture age related changes in the pulse waveform. This has significant implications for assessing vascular health unobtrusively,

continuously and at scale. Consumer wearables that utilize PPG-based assessments may be instrumental in testing strategies to delay, or reverse age-associated increases in arterial stiffness by providing timely feedback about the effect of interventions. Furthermore, identifying individuals with early or accelerated vascular aging before overt CVD develops (particularly among younger or middle-aged at-risk adults who do not cross traditional treatment thresholds) could allow for pre-emptive interventions. Sleep tracking wearables in particular, offer significant advantages because sleep period is less prone motion artifacts and age-related changes in PPG waveform are more pronounced during sleep [36]. Nocturnal dipping pattern in arterial stiffness [45,46] may enable more precise characterization of vascular health compared to episodic daytime measurements, but this remains to be tested.

Wearable vascular age estimation targets middle-aged persons interested in health preservation

While this work builds on associations between pulse waveform morphology, aging, and arterial stiffness to explore wearable-based vascular age assessment, there are two important points to note. The first concerns the disproportionate contribution of younger and mid-age persons to the data that is intended to inform about ‘vascular aging’. The distribution of users reported here is typical of the user base of wearable trackers, i.e., mid-aged and younger persons. These persons often purchase devices for health improvement or preservation and stand to gain the most from desirable lifestyle modifications in contrast to older adults who may already have accumulated pathology. Second, the CNN model’s performance and the proportional bias could potentially be improved by training on a larger, more demographically and clinically diverse population. However, proportional bias, where prediction error increases systematically with the magnitude of the measured variable, is a well-documented phenomenon in organ age prediction studies using regression-based deep learning models [47,48]. The age dependence of the raw age gap (raw- Δ Age) can be attenuated by regressing raw- Δ Age on chronological age to adjust for regression-to-the-mean bias [35,47–49]. This adjustment is particularly relevant when assessing associations between organ age estimates (e.g., vascular age) and clinical outcomes. Adjusted Δ Age values are shown in Fig. 4c to illustrate the reduction of proportional bias and to visualize variability in age-independent Δ Age values.

Relatedly, it is crucial that deviations from chronological age should not be viewed solely as a prediction error, as our findings suggest they may reflect inter-individual differences in vascular age that relate to true differences in cardiovascular risk. Even in our predominantly healthy sample, BP tended to increase with increasing Δ Age (Fig. 6) and the relationship was more pronounced for SBP. We refrain from over-interpreting these results as our sample had restricted range of BP values. These effect sizes could be larger in populations at higher cardiovascular risk. Testing PPG-based vascular age prediction against the cfPWV-based approach and in less healthy participants is an important direction for future work.

Data from multiple nights would be helpful to assess the reliability and stability of the current prediction results, as well as to evaluate possible changes in arterial stiffness in accordance to lifestyle modifications. In cases where there were 2 nights from the same participant, the correlation between estimated vascular ages between night 1 and night 2 was strong for both the Fingertip and Ring devices, although the Ring showed slightly lower correlation (S6 Fig). Currently, vascular age is clinically assessed during a single clinic visit. Understanding how PPG waveform characteristics, and by extension, vascular age, fluctuates from measurement to measurement over a short time interval remains an important question.

Conclusion

In summary, in an aging population, scalable methods to identify individuals with early or accelerated vascular aging is essential. We demonstrate that PPG signals from consumer wearable can reasonably estimate vascular age, facilitating scalable monitoring of vascular health in the field. Given the strong link between arterial stiffness and disease, the findings of this study hold great promise for preventive healthcare.

Methods

Ethics declaration

All procedures were approved by the Institutional Review Board of the National University of Singapore (NUS-IRB-2020–463), and the protocol was in accordance with the principles in the Declaration of Helsinki. All participants signed written informed consent before commencing the study.

Study design and participants

Nominally healthy adults aged between 20 and 70 were recruited for two separate overnight sleep studies conducted one year apart [36,50]. A total of 165 healthy adults provided PPG data, of whom 160 were included in the analysis [(78 (49%) males; median (IQR) age 31(23), Table 1)]. Participants were free from pre-existing sleep, neurological or psychiatric disorders, excessive daytime sleepiness (Epworth Sleepiness Scale 43 scores > 10), not on wake-promoting medications, had a body mass index (BMI) < 35 kg/m² and habitually slept more than 5 hours/night.

Demographic information, height, weight and office blood pressure (BP), were collected during a daytime briefing session prior to their overnight sleep sessions. Office BP was measured three times per participant, and the average of the three readings was used as the final BP value. In addition, participants completed questionnaires regarding their history of medically diagnosed hypertension and current medication use. Informed consent was obtained during the briefing session.

Based on self-reports, 2 participants had hypertension, with 1 on antihypertensive medication. Only 4 out of 160 participants met the Singapore hypertension criteria (SBP ≥ 140 mmHg or DBP ≥ 90 mmHg) based on office BP measurements (S7 Fig).

Participants slept overnight in the lab while polysomnography (PSG), fingertip photoplethysmography (PPG) and wearable ring data were collected simultaneously. Lights off and lights on times were assigned according to the participant's habitual bed and wake times.

Data acquisition

Polysomnography (PSG)

As part of the polysomnography (PSG) setup (SOMNOmedics GmbH, Randersacker, Germany), electroencephalography was recorded from two channels (C3 and C4) according to the international 10–20 system, and referenced to the contralateral mastoids. The common ground and reference electrodes were placed at Fpz and Cz, respectively. Electrooculography (EOG; right and left outer canthi), submental electromyography (EMG), thoracic breathing effort, electrocardiography (ECG) and plethysmography (PPG) signals were recorded. The sampling rate of EEG, ECG, and PPG was 256 Hz. PSG recordings for the entire night were segmented into 30-second epochs between “lights off” and “lights on” markers (denoting when participants were in bed) for PPG pulse extraction (see below).

Fingertip pulse oximeter

The fingertip PPG signal was recorded using the pulse oximeter probe of a SOMNOtouch device (SOMNOmedics GmbH, Randersacker, Germany) which operates on a transmission mode using red (660 nm) and infrared (880nm) light emitting diodes (LEDs) [51]. Sampling rate was 256 Hz. The PPG sensor was placed on the finger that provided the best fit (often the index finger) of the non-dominant hand.

Consumer Wearable Ring

The Oura Ring Gen 3 (Oura Ring Inc, Oulu, Finland) is a commercially available sleep, pulse rate and activity tracker. It employs multiple infrared (900 nm) LEDs on partially transmissive and partially reflective modes concurrently to collect

PPG during sleep [41]. For this study, Oura Ring Inc provided “memory rings” with the same sensors as the commercially available Oura Ring, but with additional flash memory to record minimally processed sensor data. The ring was worn on the non-dominant hand but on a different finger (than the fingertip probe) that provided the best fit. Sampling rate of the PPG was 50 Hz. [Fig 1](#) illustrates placement of devices and the PPG collection protocol.

Pulse waveform analysis

Pulse waveform and feature extraction were applied to the night-level data of each participant. After bandpass filtering (0.05 - 20 Hz, 4th order Chebyshev) and detection of large motion artefacts (via signal envelope based thresholding), the PPG signal was segmented into 30-second windows between light off and on times. Within these 30 sec windows, signal segments were analysed to find individual pulse waveforms and extract feature information.

Initially, pulses (onset times) were detected using the `qppg.m` function from The PhysioNet Cardiovascular Signal Toolbox [52]. Artefactual onset detections were automatically removed based on physiological plausibility criteria: 1) Lower and upper limits of onset-to-onset duration were set to 0.4 sec and 2 sec, 2) Maximum acceptable change in peak-to-peak duration between consecutive pulses was set to 40%. Baseline drift on the PPG segment was removed using cubic spline [53,54]. Individual pulses were normalized in width into 200 equally spaced intervals by cubic spline interpolation [55]. Pulse amplitude was normalized to a range of 0–1. Only pulses that passed the signal quality check were used in the feature extraction step and age prediction model (See [S8 Fig](#)).

Fiducial points on the pulse wave (onset, offset, systolic peak, diastolic peak, and the dicrotic notch) were identified using a custom algorithm that used the first, second and third derivatives of the pulse together with peak information from the fitted gaussians on the template (See [S9 Fig](#)). Using fiducial points, we derived the following indices, which were found to be associated with age: *CT* (*crest time*) as the time from onset to systolic peak [15]; *dT* as the time difference between systolic and diastolic peaks [16]; *RI* (*reflection index*) as the ratio between diastolic and systolic peak amplitudes [22]. To account for the influence of heart rate (HR) variations, individual pulses were normalized in width to 200 equally spaced intervals using cubic spline interpolation [36], and unless otherwise stated, results for duration-normalized pulses and PPG features (*CT*, *dT* and *RI*) are presented in the main text, while results for un-normalized pulses (*CT* and *dT* with duration in seconds) are provided in the supplementary for comparison with previous studies. Since *RI* is a ratio of amplitudes, normalization did not affect values obtained. The median value of PPG features was calculated for each 30-second window, and used in paired analysis.

Data inclusion

Pre-processed night-level data was grouped by participant and concatenated into a single participant-level data frame, as some participants had data from two sleep sessions [36]. For waveform similarity and PPG feature analysis (feature-based model), Fingertip and Oura data were paired at the 30-second window level, with twenty pairs randomly selected per participant. Participant-level data for each sensor was averaged across paired windows, resulting in 158 participants being included. The median (IQR) number of pulses per participant (used in waveform comparison and PPG-features analysis) was 364 (152) for Fingertip and 367 (139) for Ring ([S10 Fig-b](#)).

For the deep-learning model, number of pulses was standardized by randomly selecting 370 pulses per participant from each device. This value was chosen based on inspection of the per-participant pulse count distributions for both sensors and to ensure consistency with the PPG feature-based analyses. This resulted in a dataset with 160 participants for the deep learning model (See [S10 Fig-a](#))

Vascular age estimation (regression model)

To assess the accuracy of vascular age prediction using PPG features alone, we built multiple linear regression models with *CT*, *dT*, and *RI* as predictors and age as dependent variable. A 10-fold cross-validation approach was used, with a

90/10 train-test split. Model performance was evaluated on the test set of each fold, and the results were reported as the mean performance across all 10 folds.

Vascular age estimation (deep-learning model)

The deep learning framework consisted of a 1D convolutional neural network (CNN) followed by fully connected (FC) layers. We used a compact architecture (two convolutional layers followed by two FC layers) to limit model capacity and reduce overfitting risk given the participant-level sample size ($N = 160$). This design was informed by prior work [34] which used fixed-length PPG pulse inputs, moderate kernel sizes with stride 1, and a 1024-unit FC layer with dropout, and explored different convolutional depths. In our exploratory experiments, deeper variants (3–4 convolutional layers) did not improve cross-validated validation performance; therefore, we retained the two-layer model for robustness and reproducibility. The network input was a single-channel PPG pulse resampled from onset to offset into a fixed-length 200×1 vector. The two convolutional layers used 16 filters (kernel size 11) and 32 filters (kernel size 9), with stride = 1 and no pooling, followed by two FC layers (1024 units) and dropout ($p = 0.2$) applied after each FC layer, and a final linear output neuron. Stacking the 11- and 9-sample kernels yields an effective receptive field of 19 samples ($\sim 9.5\%$ of the pulse), providing local context for morphology learning. ReLU activations were applied throughout (S8 Fig).

Training and optimization

A ten-fold cross-validation approach was used for model optimization and evaluation. The folds were constructed at the participant level. In each iteration, one fold (16 participants) served as the test set. The remaining nine folds were split into training and validation sets in an 8:1 ratio, yielding 128 participants in the training set and 16 participants in the validation set. Care was taken so that waveforms of the same participant were exclusively assigned to either training, validation or test set within each fold.

Hyperparameter optimization was conducted separately for each fold's validation set. A heuristic grid search was performed for each fold, exploring various hyperparameter configurations listed in S6 Table. For the SGD optimizer, the gradient decay rates (β_1 and β_2) were 0.9 and 0.999 and the weight decay value for both Adam and SGD optimizers was 1×10^{-7} . The final model performance was evaluated on the test set of each fold using the optimal hyperparameter set of that fold.

grad-cam visualisation

Grad-CAM (Gradient-weighted Class Activation Mapping) is a technique for visualizing the regions of an input that significantly influence a CNN's predictions [56]. Heatmaps were generated to identify the regions of the PPG waveform most relevant to the model's predictions. These heatmaps were averaged across all pulses and stratified by different age groups to examine age-related patterns in the PPG signals.

Statistical analysis

Variables were summarized as mean \pm SD or median (IQR) based on their distribution, and appropriate parametric or non-parametric tests were applied. Fisher's z-test was used to compare linear correlation coefficients. As part of sensitivity analyses, random sampling of paired windows was repeated for 100 times, and relationship between age and PPG-features was evaluated for each cycle. This was done to show that randomly sampled windows were representative of participant-mean and not dominated by any sleep stage (particularly as deep sleep tends to dominate in the earlier part of the night). To assess whether the performance metrics (MAE, RMSE, R^2 , and correlation coefficient) differed significantly between Fingertip and Ring across the 10-fold cross-validation results, we employed the corrected resampled t-test [57,58]. Bonferroni correction was applied for multiple comparisons. In Bland Altman analysis, raw bias or raw- Δ Age was

defined as the difference between the estimated vascular age and chronological age. The limits of agreement (LoA) were defined as mean bias $\pm 1.96 \times$ SD of the differences. A linear regression model was fitted with raw- Δ Age as the dependent variable and chronological age as the independent variable. The residuals from this regression were used as age-adjusted Δ Age values [47,48]. Lastly, age-adjusted Δ Age values were grouped into tertiles for both Fingertip and Ring, and their associations with BP were examined using linear regression models including age, sex, and BMI as covariates. Bonferroni correction was applied to account for multiple comparisons.

Code Availability

PPG pulse waveform and feature extraction were conducted in MATLAB version R2023b (The Math Works, Inc., Natick, MA) using custom algorithms. The signal quality criteria and data exclusion rules were identical for both the fingertip and the ring PPG. The deep learning model was implemented and executed using Python 3.10.15, PyTorch 2.0.1 with CUDA 11.7 (compiler version of V11.7.64.) Model training and validation were conducted on a high-performance computing (HPC) system equipped with four NVIDIA GeForce RTX 3090 GPUs. The GPU setup was managed by NVIDIA-SMI (Driver Version: 550.54.14). Code used in this study can be accessed at <https://github.com/SCL-NUS/ppg-vascularage-ring>.

Supporting information

S1 Fig. Distributions of PPG features (duration normalized) for Fingertip and Ring, across participants. RI showed the largest difference in magnitude, with a clear separation between devices, while CT and dT were overlapping. Red color is used for Ring, blue is for Fingertip. CT: Crest time, dT: distance between systolic and diastolic peaks, RI: Reflection index.

(DOCX)

S2 Fig. Agreement between PPG features from the fingertip sensor and the ring. The scatter plots for Fingertip and Ring PPG features are on the left column, while Bland-Altman plots are on the right. Each color represents a unique participant. (r: pearson's correlation coefficient, ccc: Lin's correlation coefficient), CT: Crest time, dT: distance between systolic and diastolic peaks, RI: Reflection index.

(DOCX)

S3 Fig: Distribution of correlation coefficients between age and PPG features for 100 different subsets of 20 randomly sampled windows used to calculate participant means. Vertical dashed lines indicate group means, and the text above the lines shows mean (SD). Blue represents Fingertip, and red represents Ring. CT: Crest time; dT: distance between systolic and diastolic peaks; RI: Reflection index.

(DOCX)

S4 Fig. Prediction accuracy comparison between devices. Results with corrected resampled paired t-test for dependencies between 10 folds. P-values are corrected for multiple comparisons.

(DOCX)

S5 Fig. Comparison of model performance between CNN and regression models for Fingertip (A) and Ring (B). Each dot represents a fold. REG: Regression.

(DOCX)

S6 Fig. Correlation of estimated vascular age between Night 1 and Night 2 for Fingertip (A) and Ring (B). Each dot represents a subject. Only 63 participants had 2 nights of data (N=63). The trained models and the original participant assignments to the training, validation, and test sets were kept unchanged. New test sets were created by selecting participants with

two nights of data from each fold's test set and randomly sampling 150 pulses from each night. The trained models were then applied separately to the Night 1 and Night 2 data to predict vascular age. r : Pearson correlation coefficient.

(DOCX)

S7 Fig. Distribution of systolic (SBP) and diastolic (DBP) blood pressure values among participants. Each dot represents a participant, with color indicating chronological age. Red dashed lines indicate blood pressure values for hypertension as defined in Singapore ($SBP \geq 140$ mmHg, $DBP \geq 90$ mmHg), the red rectangle in the top-right corner highlights the hypertension range.

(DOCX)

S8 Fig. Summary of analysis pipeline. Preprocessing and age prediction using deep learning model are illustrated. QC: Quality Check, FC: Fully Connected.

(DOCX)

S9 Fig. Summary of fiducial point detection algorithm using pulse and its derivatives. Fiducial points are detected as follows: Onset: 1st sample on the waveform. Offset: Last sample on the waveform. Systolic peak: Point where 1st derivative crosses zero in positive to negative direction for the 1st time. Estimated diastolic peak: The peak of the second gaussian (which was fitted during template creation) was used as an estimated diastolic peak by adding %10 of it's distance from the onset. Dicrotic notch: In the 3rd derivative signal, the nearest zero-crossing in the positive-to-negative direction closest to the estimated diastolic peak. Real diastolic peak: In the 1st derivative signal, the positive-to-negative zero-crossing within the segment between the dicrotic notch and the estimated diastolic peak.

(DOCX)

S10 Fig. Distribution of total number of pulses. a. After preprocessing, 165 participants had at least one 30-second window of high-quality data from both Fingertip (blue) and Ring (red), before applying data inclusion criteria. Dashed black line marks the number of pulses included into age prediction model (370 pulses). For the included 160 participants (with at least 370 pulses from each device), the median (IQR) number of total pulses per participant was 11,988 (11,092) from Fingertip and 11,727 (10,000) from Ring. b. Distribution of number of pulses included into waveform comparison across 158 participants for Fingertip (blue) and Ring (red). The median (IQR) number of pulses per participant (used in waveform comparison and PPG-features analysis) was 364 (152) for Fingertip and 367 (139) for Ring.

(DOCX)

S1 Table. Summary of PPG-features (un-normalized duration, in seconds). When PPG features were not-normalized for duration, CT (seconds) was significantly higher in the ring, while values for dT (seconds) were similar.

(DOCX)

S2 Table. Agreement between un-normalized PPG-features (in seconds). Bias is calculated as the difference between the ring and the fingertip sensor. LoA refers to Limits of Agreement. CT: Crest time, dT: distance between systolic and diastolic peaks, PW: Pulse width.

(DOCX)

S3 Table. Regression models to predict CT, dT and RI for the fingertip sensor and the ring.

(DOCX)

S4 Table. Age prediction performance of the PPG-based regression model using the fingertip sensor and the ring.

(DOCX)

S5 Table. Prediction performance for all test sets for Fingertip and Ring.

(DOCX)

S6 Table. Hyperparameter values used in optimization and evaluation.
(DOCX)

Author contributions

Conceptualization: Gizem Yilmaz, Shohreh Ghorbani, Ju Lynn Ong, Hosein Aghayan Golkashani.

Data curation: Gizem Yilmaz, Shohreh Ghorbani.

Formal analysis: Gizem Yilmaz, Shohreh Ghorbani.

Funding acquisition: Michael W. L. Chee.

Methodology: Gizem Yilmaz, Shohreh Ghorbani, Ju Lynn Ong, Chen Zhang, B. T. Thomas Yeo.

Project administration: Gizem Yilmaz, Ju Lynn Ong.

Resources: Michael W. L. Chee.

Supervision: Chen Zhang, B. T. Thomas Yeo, Michael W. L. Chee.

Validation: Gizem Yilmaz.

Visualization: Gizem Yilmaz, Shohreh Ghorbani.

Writing – original draft: Gizem Yilmaz, Shohreh Ghorbani, Ju Lynn Ong, Hosein Aghayan Golkashani, B. T. Thomas Yeo, Michael W. L. Chee.

Writing – review & editing: Gizem Yilmaz, Shohreh Ghorbani, Ju Lynn Ong, Hosein Aghayan Golkashani, Chen Zhang, B. T. Thomas Yeo, Michael W. L. Chee.

References

1. Mensah GA, Fuster V, Murray CJL, Roth GA, Mensah GA. Global burden of cardiovascular diseases and risks, 1990-2022. *Journal of the American College of Cardiology*. 2023;82(25):2350–473. <https://doi.org/10.1016/j.jacc.2023.11.007>
2. Niiranen TJ, Lyass A, Larson MG, Hamburg NM, Benjamin EJ, Mitchell GF. Prevalence, correlates, and prognosis of healthy vascular aging in a western community-dwelling cohort. *Hypertension*. 2017;70(2):267–74. <https://doi.org/10.1161/HYPERTENSIONAHA.117.09026>
3. Bruno RM, Nilsson PM, Engström G, Wadström BN, Empana JP, Boutouyrie P. Early and supernormal vascular aging. *Hypertension*. 2020;76(5):1616–24. <https://doi.org/10.1161/HYPERTENSIONAHA.120.14971>
4. Climie RE, Alastruey J, Mayer CC, Schwarz A, Laucyte-Cibulskiene A, Voicehovska J, et al. Vascular ageing: moving from bench towards bedside. *Eur J Prev Cardiol*. 2023;30(11):1101–17. <https://doi.org/10.1093/eurjpc/zwad028> PMID: 36738307
5. Mitchell GF, Parise H, Benjamin EJ, Larson MG, Keyes MJ, Vita JA. Changes in arterial stiffness and wave reflection with advancing age in healthy men and women. *Hypertension*. 2004;43(6):1239–45. <https://doi.org/10.1161/01.HYP.0000128420.01881.a>
6. Mitchell GF, Wang N, Palmisano JN, Larson MG, Hamburg NM, Vita JA, et al. Hemodynamic Correlates of Blood Pressure Across the Adult Age Spectrum. *Circulation*. 2010;122(14):1379–86. <https://doi.org/10.1161/circulationaha.109.914507>
7. McEniery CM, Yasmin Maki-Petaja KM, McDonnell BJ, Munnery M, Hickson SS, et al. The Impact of Cardiovascular Risk Factors on Aortic Stiffness and Wave Reflections Depends on Age. *Hypertension*. 2010;56(4):591–7. <https://doi.org/10.1161/HYPERTENSIONAHA.110.156950>
8. Boutouyrie P, Chowienczyk P, Humphrey JD, Mitchell GF. Arterial Stiffness and Cardiovascular Risk in Hypertension. *Circ Res*. 2021;128(7):864–86. <https://doi.org/10.1161/CIRCRESAHA.121.318061> PMID: 33793325
9. Nowak KL, Rossman MJ, Chonchol M, Seals DR. Strategies for Achieving Healthy Vascular Aging. *Hypertension*. 2018;71(3):389–402. <https://doi.org/10.1161/HYPERTENSIONAHA.117.10439> PMID: 29311256
10. Rossman MJ, LaRocca TJ, Martens CR, Seals DR. Healthy lifestyle-based approaches for successful vascular aging. *J Appl Physiol* (1985). 2018;125(6):1888–900. <https://doi.org/10.1152/jappphysiol.00521.2018> PMID: 30212305
11. Gómez-Sánchez L, González-Falcon D, Llamas-Ramos R, Rodríguez MC, Rodríguez-Sánchez E, García-Ortiz L. The relationship between healthy vascular aging with the Mediterranean diet and other lifestyles in the Spanish population: The EVA study. *Nutrients*. 2024;16(15). <https://doi.org/10.3390/nu16152565>
12. Nilsson PM, Boutouyrie P, Laurent S. Vascular Aging. *Hypertension*. 2009;54(1):3–10. <https://doi.org/10.1161/HYPERTENSIONAHA.109.129114>
13. Mitchell GF, Rong J, Larson MG, Korzinski TJ, Xanthakis V, Sigurdsson S, et al. Vascular age assessed from an uncalibrated, noninvasive pressure waveform by using a deep learning approach: the AI-vascularage model. *Hypertension*. 2023;HYPERTENSIONAHA.123.21638. <https://doi.org/10.1161/HYPERTENSIONAHA.123.21638>

14. Hughes A, Shandhi MMH, Master H, Dunn J, Brittain E. Wearable Devices in Cardiovascular Medicine. *Circulation Research*. 2023;132(5):652–70. <https://doi.org/10.1161/CIRCRESAHA.122.322389>
15. Allen J, O'Sullivan J, Stansby G, Murray A. Age-related changes in pulse risetime measured by multi-site photoplethysmography. *Physiol Meas*. 2020;41(7):074001. <https://doi.org/10.1088/1361-6579/ab9b67> PMID: 32784270
16. Millasseau SC, Kelly RP, Ritter JM, Chowienczyk PJ. Determination of age-related increases in large artery stiffness by digital pulse contour analysis. *Clin Sci (Lond)*. 2002;103(4):371–7. <https://doi.org/10.1042/cs1030371> PMID: 12241535
17. Svedmyr S, Zou D, Sommermeyer D, Ficker JH, Randerath W, Fietze I, et al. Vascular stiffness determined from a nocturnal digital pulse wave signal: association with sleep, sleep-disordered breathing, and hypertension. *J Hypertens*. 2016;34(12):2427–33. <https://doi.org/10.1097/HJH.0000000000001111> PMID: 27607460
18. Hibbing PR, Khan MM. Raw Photoplethysmography as an Enhancement for Research-Grade Wearable Activity Monitors. *JMIR Mhealth Uhealth*. 2024;12:e57158. <https://doi.org/10.2196/57158> PMID: 39331461
19. McVeigh GE, Bratteli CW, Morgan DJ, Alinder CM, Glasser SP, Finkelstein SM, et al. Age-Related Abnormalities in Arterial Compliance Identified by Pressure Pulse Contour Analysis. *Hypertension*. 1999;33(6):1392–8. <https://doi.org/10.1161/01.hyp.33.6.1392>
20. Alastruey J, Charlton PH, Bikia V, Paliakaite B, Hametner B, Bruno RM, et al. Arterial pulse wave modeling and analysis for vascular-age studies: a review from VascAgeNet. *Am J Physiol Heart Circ Physiol*. 2023;325(1):H1–29. <https://doi.org/10.1152/ajpheart.00705.2022> PMID: 37000606
21. Alty SR, Angarita-Jaimes N, Millasseau SC, Chowienczyk PJ. Predicting arterial stiffness from the digital volume pulse waveform. *IEEE Trans Biomed Eng*. 2007;54(12):2268–75. <https://doi.org/10.1109/tbme.2007.897805> PMID: 18075043
22. Brillante DG, O'Sullivan AJ, Howes LG. Arterial stiffness indices in healthy volunteers using non-invasive digital photoplethysmography. *Blood Press*. 2008;17(2):116–23. <https://doi.org/10.1080/08037050802059225> PMID: 18568701
23. Lin W-H, Zheng D, Li G, Chen F. Age-Related Changes in Blood Volume Pulse Wave at Fingers and Ears. *IEEE J Biomed Health Inform*. 2024;28(9):5070–80. <https://doi.org/10.1109/JBHI.2023.3282796> PMID: 37276108
24. Pilt K, Meigas K, Kõõts K, Viigimaa M. Photoplethysmographic signal rising front analysis for the discrimination of subjects with increased arterial ageing; pp. 309–314. *PEAS*. 2014;63(3):309–14. <https://doi.org/10.3176/proc.2014.3.03>
25. Zhang Y-L, Zheng Y-Y, Ma Z-C, Sun Y-N. Radial pulse transit time is an index of arterial stiffness. *Hypertens Res*. 2011;34(7):884–7. <https://doi.org/10.1038/hr.2011.41> PMID: 21593741
26. Charlton PH, Paliakaite B, Pilt K, Bachler M, Zanelli S, Kulin D, et al. Assessing hemodynamics from the photoplethysmogram to gain insights into vascular age: a review from VascAgeNet. *Am J Physiol Heart Circ Physiol*. 2022;322(4):H493–522. <https://doi.org/10.1152/ajpheart.00392.2021> PMID: 34951543
27. Ahn JM. New Aging Index Using Signal Features of Both Photoplethysmograms and Acceleration Plethysmograms. *Healthc Inform Res*. 2017;23(1):53–9. <https://doi.org/10.4258/hir.2017.23.1.53> PMID: 28261531
28. Bortolotto LA, Blacher J, Kondo T, Takazawa K, Safar ME. Assessment of vascular aging and atherosclerosis in hypertensive subjects: second derivative of photoplethysmogram versus pulse wave velocity. *Am J Hypertens*. 2000;13(2):165–71. [https://doi.org/10.1016/s0895-7061\(99\)00192-2](https://doi.org/10.1016/s0895-7061(99)00192-2) PMID: 10701816
29. Huotari M, Yliaska N, Lantto V, Määttä K, Kostamovaara J. Aortic and arterial stiffness determination by photoplethysmographic technique. *Proced Chem*. 2009;1:1243–6.
30. Shin H. XGBoost Regression of the Most Significant Photoplethysmogram Features for Assessing Vascular Aging. *IEEE J Biomed Health Inform*. 2022;26(7):3354–61. <https://doi.org/10.1109/JBHI.2022.3151091> PMID: 35157602
31. Tang Q, Tao C, Pan Z, Wang G, Liu K, Pan Z, et al. A novel method for vascular age estimation via pressure pulse wave of radial artery. *Biomedical Signal Processing and Control*. 2022;78:103904. <https://doi.org/10.1016/j.bspc.2022.103904>
32. Chiarelli AM, Bianco F, Perpetuini D, Bucciarelli V, Filippini C, Cardone D, et al. Data-driven assessment of cardiovascular ageing through multi-site photoplethysmography and electrocardiography. *Med Eng Phys*. 2019;73:39–50. <https://doi.org/10.1016/j.medengphy.2019.07.009> PMID: 31358395
33. Dall'Olio L, Curti N, Remondini D, Safi Harb Y, Asselbergs FW, Castellani G, et al. Prediction of vascular aging based on smartphone acquired PPG signals. *Sci Rep*. 2020;10(1):19756. <https://doi.org/10.1038/s41598-020-76816-6> PMID: 33184391
34. Shin H, Noh G, Choi BM. Photoplethysmogram based vascular aging assessment using the deep convolutional neural network. *Sci Rep*. 2022;12(1):11377. <https://doi.org/10.1038/s41598-022-15240-4>
35. Miller AC, Futoma J, Abbaspourzad S, Heinze-Deml C, Emrani S, Shapiro I, et al. A wearable-based aging clock associates with disease and behavior. *Nat Commun*. 2025;16(1):9264. <https://doi.org/10.1038/s41467-025-64275-4> PMID: 41115881
36. Yilmaz G, Ong JL, Ling LH, Chee MWL. Insights into vascular physiology from sleep photoplethysmography. *Sleep*. 2023. <https://doi.org/10.1093/sleep/zsad172>
37. Strauch B, de Moura W. Arterial system of the fingers. *J Hand Surg Am*. 1990;15(1):148–54. [https://doi.org/10.1016/s0363-5023\(09\)91123-6](https://doi.org/10.1016/s0363-5023(09)91123-6) PMID: 2299156
38. Hartmann V, Liu H, Chen F, Qiu Q, Hughes S, Zheng D. Quantitative comparison of photoplethysmographic waveform characteristics: effect of measurement site. *Frontiers in Physiology*. 2019. <https://doi.org/10.3389/fphys.2019.00198>

39. Warrender WJ, Salmons HI, Pham P, Watkins C, Jones C, Rivlin M. Physiological Nocturnal Hand Swelling: A Prospective Evaluation of Healthy Volunteers. *The Journal of Hand Surgery*. 2019 Mar 1;44(3):245.e1–245.e5. <https://doi.org/10.1016/j.jhsa.2018.05.032>
40. Sirkä J-P, Panula T, Kaisti M. Investigating the impact of contact pressure on photoplethysmograms. *Biomedical Engineering Advances*. 2024;7:100123. <https://doi.org/10.1016/j.bea.2024.100123>
41. Altini M, Kinnunen H. The promise of sleep: A multi-sensor approach for accurate sleep stage detection using the Oura ring. *Sensors*. 2021;21(13):13. <https://doi.org/10.3390/s21134302>
42. Jang D-G, Park S-H, Hahn M. Enhancing the pulse contour analysis-based arterial stiffness estimation using a novel photoplethysmographic parameter. *IEEE J Biomed Health Inform*. 2015;19(1):256–62. <https://doi.org/10.1109/JBHI.2014.2306679> PMID: 25561448
43. Park J, Shin H. Vascular aging estimation based on artificial neural network using photoplethysmogram waveform decomposition: Retrospective cohort study. *JMIR Medical Informatics*. 2022;10(3):e33439. <https://doi.org/10.2196/33439>
44. Millasseau SC, Ritter JM, Takazawa K, Chowienczyk PJ. Contour analysis of the photoplethysmographic pulse measured at the finger. *J Hypertens*. 2006;24(8):1449–56. <https://doi.org/10.1097/01.hjh.0000239277.05068.87> PMID: 16877944
45. Dhaun N, Moorhouse R, MacIntyre IM, Melville V, Oosthuyzen W, Kimmitt RA, et al. Diurnal variation in blood pressure and arterial stiffness in chronic kidney disease: the role of endothelin-1. *Hypertension*. 2014;64(2):296–304. <https://doi.org/10.1161/HYPERTENSIONAHA.114.03533> PMID: 24890823
46. Gaffey AE, Walenczyk KM, Schwartz JE, Hall MH, Burg MM. Ecologically Assessed Sleep Duration and Arterial Stiffness in Healthy Men and Women. *Psychosom Med*. 2024;86(9):740–7. <https://doi.org/10.1097/PSY.0000000000001335> PMID: 39225340
47. Le TT, Kuplicki RT, McKinney BA, Yeh H-W, Thompson WK, Paulus MP, et al. A Nonlinear Simulation Framework Supports Adjusting for Age When Analyzing BrainAGE. *Front Aging Neurosci*. 2018;10:317. <https://doi.org/10.3389/fnagi.2018.00317> PMID: 30405393
48. Smith SM, Vidaurre D, Alfaro-Almagro F, Nichols TE, Miller KL. Estimation of brain age delta from brain imaging. *Neuroimage*. 2019;200:528–39. <https://doi.org/10.1016/j.neuroimage.2019.06.017> PMID: 31201988
49. Tian YE, Cropley V, Maier AB, Lautenschlager NT, Breakspear M, Zalesky A. Heterogeneous aging across multiple organ systems and prediction of chronic disease and mortality. *Nat Med*. 2023;29(5):1221–31. <https://doi.org/10.1038/s41591-023-02296-6> PMID: 37024597
50. Ong JL, Golkashani HA, Ghorbani S, Wong KF, Chee NIYN, Willoughby AR, et al. Selecting a sleep tracker from EEG-based, iteratively improved, low-cost multisensor, and actigraphy-only devices. *Sleep Health*. 2024;10(1):9–23. <https://doi.org/10.1016/j.sleh.2023.11.005> PMID: 38087674
51. Somnomedics-SOMNOtouch™ RESP Polygraphy - When size matters. https://somnomedics.de/en/solutions/sleep_diagnosics/polygraphy-devices/somnotouch-resp/ 2025 February 24.
52. Vest AN, Da Poian G, Li Q, Liu C, Nemati S, Shah AJ, et al. An open source benchmarked toolbox for cardiovascular waveform and interval analysis. *Physiol Meas*. 2018;39(10):105004. <https://doi.org/10.1088/1361-6579/aae021> PMID: 30199376
53. Yang L, Zhang S, Li X, Yang Y. Removal of Pulse Waveform Baseline Drift Using Cubic Spline Interpolation. In: 2010 4th International Conference on Bioinformatics and Biomedical Engineering, 2010. 1–3. <https://doi.org/10.1109/icbbe.2010.5516523>
54. González S, Hsieh W-T, Chen TP-C. A benchmark for machine-learning based non-invasive blood pressure estimation using photoplethysmogram. *Sci Data*. 2023;10(1):149. <https://doi.org/10.1038/s41597-023-02020-6> PMID: 36944668
55. Allen J, Murray A. Age-related changes in the characteristics of the photoplethysmographic pulse shape at various body sites. *Physiol Meas*. 2003;24(2):297–307. <https://doi.org/10.1088/0967-3334/24/2/306> PMID: 12812416
56. Selvaraju RR, Cogswell M, Das A, Vedantam R, Parikh D, Batra D. Grad-CAM: Visual Explanations from Deep Networks via Gradient-Based Localization. In: 2017 IEEE International Conference on Computer Vision (ICCV), 2017. 618–26. <https://doi.org/10.1109/iccv.2017.74>
57. Nadeau C, Bengio Y. Inference for the generalization error. *Advances in Neural Information Processing Systems*. MIT Press. 1999.
58. Bouckaert RR, Frank E. Evaluating the Replicability of Significance Tests for Comparing Learning Algorithms. *Lecture Notes in Computer Science*. Springer Berlin Heidelberg. 2004. p. 3–12. https://doi.org/10.1007/978-3-540-24775-3_3